Single-element elliptical hard x-ray micro-optics

Kenneth Evans-Lutterodt, James M. Ablett, Aaron Stein and Chi-Chang Kao

National Synchrotron Light Source, Brookhaven National Laboratory, Upton, New York, 11973

kenne@bnl.gov

Donald M.Tennant, Fred Klemens and Ashley Taylor

New Jersey Nanotechnology Consortium, Murray Hill, New Jersey, 07974

Chris Jacobsen,

Department of Physics and Astronomy, SUNY Stony Brook, Stony Brook, New York, 11794

Peter L. Gammel, Harold Huggins, Scott Ustin, Greg Bogart and Leo Ocola

Agere Systems, Allentown, Pennsylvania, 18109

Abstract: Using micro-fabrication techniques, we have manufactured a single element kinoform lens in single-crystal silicon with an elliptical profile for 12.398 keV (1Å) x-rays. By fabricating a lens that is optimized at fixed wavelengths, absorption in the lens material can be significantly reduced by removing 2π phase-shifting regions. This permits short focal length devices to be fabricated with small radii of curvatures at the lens apex. This feature allows one to obtain a high demagnification of a finite synchrotron electron source size. The reduced absorption loss also enables optics with a larger aperture, and hence improved resolution for focussing and imaging applications. Our first trial of these lenses has resulted in a one micron line focus (*fwhm*) at the National Synchrotron Light Source X13B beamline.

OCIS codes: (340.0340) X-ray optics; (220.3630) Lenses

References and Links

1. O. Hignette *et al.* in X-Ray Micro- and Nano- Focusing: Applications and Techniques II (ed. McNulty) 105-116 (SPIE, San Diego, 2001).
2. W. Yun *et al.* Nanometer focusing of hard x rays by phase zone plates. Rev. Sci. Instrum. **70**, 2238-2241 (1999).
3. C. G. Schroer *et al.* Nanofocusing parabolic refractive x-ray lenses. Appl. Phys. Lett. **82**, 1485-1487 (2003).
4. G. E. Ice. Microbeam-Forming Methods for Synchrotron Radiation. X-Ray Spectrometry **26**, 315-326 (1997).
5. P. Dhez, P. Chevallier, T. B. Lucatorto & C. Tarrio. Instrumental aspects of x-ray microbeams in the range above 1 keV. Rev. Sci. Instrum. **70**, 1907-1920 (1999).
6. L. B. Lesem, P. M. Hirsch & J. A. J. Jordan. IBM J. Res. Dev. **13**, 150 (1969).
7. J. Kirz. Phase Zone Plates for X-rays and the Extreme UV. J. Opt. Soc. Am. **64** (1974).
8. R. Gähler, J. Kalus & W. Mampe. An optical instrument for the search of a neutron charge. J. Phys. E **13**, 546-548 (1980).
9. S. Suehiro, H. Miyaji & H. Hayashi. Refractive lens for X-ray focus. Nature **352**, 385-386 (1991).
10. A. Snigirev, V. Kohn, I. Snigireva & B. Lengeler. A compound refractive lens for focusing high-energy X-rays. Nature **384**, 49-51 (1996).
11. M. A. Piestrup, J. T. Cremer, H. R. Beguiristain, C. K. Gary & R. H. Pantell. Two-dimensional x-ray focusing from compound lenses made of plastic. Rev. Sci. Instrum. **71**, 4375-4379 (2000).
12. J. T. Cremer, M. A. Piestrup, H. R. Beguiristain & C. K. Gary. Cylindrical compound refractive x-ray lenses using plastic substrates. Rev. Sci. Instrum. **70**, 3545-3548 (1999).

#2224 - $15.00 US Received March 13, 2003; Revised April 11, 2003

13. C. G. Schroer *et al.* High resolution imaging and lithography with hard x rays using parabolic compund refractive lenses. Rev. Sci. Instrum. **73**, 1640-1642 (2002).
14. B. Lengeler *et al.* A microscope for hard x rays based on parabolic refractive lenses. Appl. Phys. Lett. **74**, 3924-3926 (1999).
15. B. Lengeler *et al.* Imaging by parabolic refractive lenses in the hard X-ray range. J. Sync. Rad. **6**, 1153-1167 (1999).
16. I. Snigireva *et al.* Holographic X-ray optical elements: transition between refraction and diffraction. Nuclear Instruments & Methods in Physics Research A **467-468**, 982-985 (2001).
17. V. Aristov *et al.* X-ray refractive planar lens with minimized absorption. Appl. Phys. Lett. **77**, 4058-4060 (2000).
18. B. Nohammer, J. Hoszowska, A. K. Freund & C. David. Diamond planar refractive lenses for third and fourth generation x-ray sources. J. Sync. Rad. **10**, 168-171 (2003).
19. D. A. Buralli, G. M. Morris & J. R. Rogers. Optical performance of holographic kinoforms. Appl. Opt. **28**, 976-983 (1989).
20. B. Lengeler, J. Tümmler, A. Snigirev, I. Snigireva & C. Raven. Transmission and gain of singly and doubly focusing refractive x-ray lenses. Journal Of Applied Physics **84**, 5855-5861 (1998).
21. E. Hecht & A. Zajac. Optics (ed. Addison-Wesley) (, 1979).
22. V. Moreno, J. F. Roman & J. R. Salgueiro. High efficiency diffractive lenses: Deduction of kinoform profile. Am. J. Phys. **65**, 556-562 (1997).
23. G. Smith & D. A. Atchison. The Eye and Visual Optical Instruments (ed. Press, C. U.) (1997).
24. C. Welnak, G. J. Chen & F. Cerrina. Shadow: A Synchrotron Radiation And X-Ray Optics Simulation Tool. Nuclear Instruments & Methods in Physics Research A **347**, 344-347 (1994).
25. B. Lai, K. Chapman & F. Cerrina. SHADOW: New Developments. Nuclear Instruments & Methods in Physics Research A **266**, 544-549 (1988).
26. B. Lai & F. Cerrina. SHADOW: A Synchrotron Radiation Ray Tracing Program. Nuclear Instruments & Methods in Physics Research A **246**, 337-341 (1986).
27. C. Welnak, P. Anderson, M. Khan, S. Singh & F. Cerrina. Recent developments in SHADOW. Rev. Sci. Instrum. **63**, 865-868 (1992).
28. G. Rakowsky, D. Lynch, E. B. Blum & S. Krinsky. NSLS In-Vaccum Undulators and Mini-Beta Straights. Proceedings of the 2001 Particle Accelerator Conference **4**, 2453-2455 (2001).
29. D. Lynch & G. Rakowsky. Mechanical Design of NSLS Mini-gap Undulator (MGU). 2nd Int. Workshop on Mech. Eng. Design of Sync. Rad. Equip. and Instrum. *(MEDSI02)* (2002).
30. A. Stein *et al.* Diffractive x-ray optics using production fabrication methods. J.Vac.Sci. Technol. **B 21**, 1071-1023 (2003).
31. I. Snigireva *et al.* in X-Ray Micro- and Nano- Focusing: Applications and Techniques II (Proceedings of SPIE, San Diego, USA, 2001).

1. Introduction

There is increasing demand for materials characterization using hard x-rays with high spatial resolution. For an ideal optic, the limiting resolution in the far-field limit is close to the wavelength of the incident radiation. For hard x-ray photons ($E \geq 4$ keV), with wavelengths of the order of 1Å, the limited availability of high quality optical elements has hindered the development of imaging and focussed spot applications. Hundred nanometer resolution has recently been achieved in the hard x-ray region with advances in the fabrication of reflective mirrors [1], diffractive zone plates [2] and refractive parabolic lenses [3]. The combination of high-brightness photon beams from synchrotron radiation sources and improvements to x-ray optics [4,5] could be expected to have a revolutionary impact in research areas such as materials science, condensed matter physics, biology and nanotechnology. In this article, the properties and fabrication of a kinoform [6] refractive lens are described. The key features of this lens are the small radius of curvature, short focal length, high transmission and novel elliptical shape.

The phase-change and absorption of an electromagnetic wave as it traverses a medium can be represented in the extreme ultra-violet and x-ray regions by the complex refractive index, $n = 1 - \delta - i\beta$. The energy-dependent optical constants, δ and β, are the refractive index decrement and absorption index respectively. In the soft x-ray region ($E < 3$ keV), β can be of the same order as δ [7], making refractive optics impractical. Since absorption decreases with energy as $\sim E^{-3}$ and δ falls as $\sim E^{-2}$, the implementation of hard x-

#2224 - $15.00 US Received March 13, 2003; Revised April 11, 2003

ray refractive optics become attractive. For example, the β/δ ratio of silicon decreases ~30-fold as the x-ray energy is varied from 2 to 12.398 keV.

In contrast with visible light, hard x-rays and neutrons have a refractive index less than one in most materials. Gähler *et al*. [8] first demonstrated the focussing of neutrons with refraction, and Suehiro *et al.* first suggested that refractive optics could be used in the focussing of x-rays [9]. To effectively use refractive lenses at synchrotron radiation facilities, short focal lengths are generally required to obtain the necessary demagnification of the finite size of the electron source. For example, with a source-to-optic distance of 10 m and an electron source size of 10 μm, a lens with a focal length f = 10 cm is needed to obtain a 0.1 μm line focus. The radius of curvature of a single cylindrical lens is $R=\delta f$, and the aperture is much too small to be of practical use. A solution to this problem is to use a lens with a larger radius of curvature and to reduce the focal length by stacking N of these elements together, thus reducing the focal length to f/N . This arrangement is called a compound refractive lens (CRL) [10]. Snigirev *et al.* demonstrated the x-ray focusing properties of a drilled aluminum cylindrical refractive lens [10] and plastic systems have also been manufactured [11,12]. A further improvement in the CRL arrangement was the implementation of parabolic profiles to reduce spherical aberration [13-15]. Planar microfabrication techniques are now being applied in the creation of parabolic compound lenses in silicon and diamond [3,16-18]. Typical parameters of compound refractive lenses result in an absorption loss that increases with stacking number *N*, and an effective aperture that is limited by absorption in the thicker parts of the lens.

An attractive solution to reduce absorption loss is through Fresnel's observation that in the refractive limit ($\lambda \to 0$), the focussing properties of the lens are due to the curved profile. The removal of material but retention of the lens shape can maintain the focussing properties while significantly reducing absorption. Such lenses can be used as light condensers, but do not generally perform well in imaging applications. However, the use of monochromatic light and the deletion of material that contribute multiples of 2π phase-shifts to the incident radiation can preserve phase coherence across the optic. Imaging with a Fresnel lens now becomes possible [19]. Figure 1 shows a scanning electron microscope image of a hard x-ray Fresnel lens as used in this article (Section 3). The apex of the lens is located towards the left-hand side of Fig. 1. The step edges are clearly visible as are the spaces which represent material that has been removed (compare this with a solid element as shown in Fig. 2).

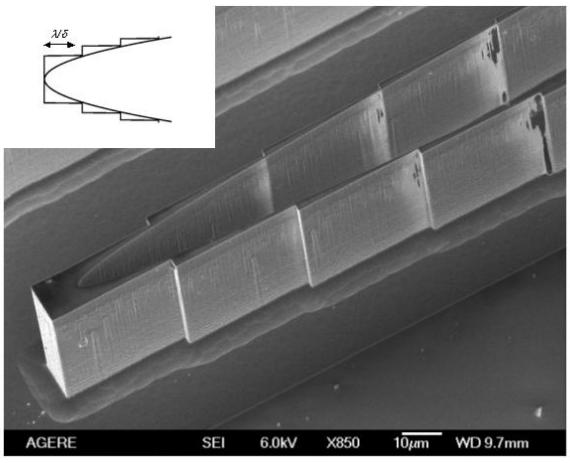

Fig. 1. Hard x-ray Fresnel lens. The profile is elliptical and steps can be seen where material that originally contributed to 2π phase-shifts has been removed. Inset: Schematic of Fresnel lens showing the length of the phase-shifting region.

#2224 - $15.00 US Received March 13, 2003; Revised April 11, 2003

The discontinuous phase-shifts imply diffractive behavior - the lens becomes a diffractive optic with an analog phase-shift across a Fresnel zone. This can be compared to the more familiar binary diffractive zone-plate which has a digital two-level phase-shift across a Fresnel zone. The properties of the lens cannot in general be understood in the refractive limit. However, if the illumination wavelength exactly matches the design wavelength, giving 2π (or multiples of 2π) phase-shifts, it behaves as a refractive optic with higher transmission. The thickness of the step is determined by phase matching conditions just inside and outside this region. The phase difference introduced by the lens medium is $2\pi\delta x/\lambda$, where x is the distance that the x-rays travel through the lens. This phase matching condition results in a step thickness of λ/δ as shown in Fig. 1 (inset). The resulting lens profile near the extrema of the optic will be triangular shaped, and will have an average thickness of $0.5\lambda/\delta$ leading to an average loss of $e^{-2\pi\frac{\beta}{\delta}}$. Thus, absorption no longer limits the aperture of the lens. It now becomes possible to choose radii of curvature consistent with shorter focal lengths and use a single element rather than a compound refractive lens system.

In order to illustrate the relative benefits of this Fresnel geometry as compared with a compound circular lens, we estimate the total amount of material required to produce a focal length of 0.15m with an aperture of 100 microns with silicon at a wavelength of 1 Å. We find that this requires 50 compound lenses, and by simple geometry this gives a projected transmission of $\approx$ 65%. In contrast, the Fresnel lens has segments which are asymptotically triangularly shaped, and leads to a transmission ~94%. In fact the compound lens will have an aperture that is smaller than the nominal physical aperture due to absorption in the thicker parts, and as a result will have poorer resolution.

Most of the important length scales found in these refractive lenses naturally fall into the range for conventional micro-electronics fabrication techniques; the step thickness can be of order 10 μm, and the radius of curvature can be of order 1 μm. Furthermore, in exactly the same manner as for binary zone plates, the size of the smallest feature at the extrema of the lens is directly proportional to the lens resolution. Electron beam writing is capable of creating the required sub-micron resolution features in a resist. Using micro-fabrication techniques allows the writing and etching of curvatures that would be difficult to manufacture otherwise [20]. A single element with the minimum thickness of λ/δ minimizes the loss in this type of lens, and the loss is independent of curvature. The flexibility of electron beam writing allows an important question to be raised; what is the optimal shape for a refractive lens for the case when the refractive index of the lensing medium is less than that of the surroundings? We note that for conventional optics, where the lens refractive index is larger than the surrounding medium, the ideal parallel beam to point converter shape is a hyperbola [21].

2. Single-element refractive geometry

In this section we show that an ellipse is the ideal shape for a single-element refractive lens. Consider the functional form of a planar concave lens operating in the x-ray region where the real part of the refractive index of the lens medium is $n' < 1$ (Fig. 2). Parallel rays traveling in air/vacuum ($n = 1$) are incident on the planar side of the lens, and are not refracted. The geometry is arranged such that the lens apex is located on the optical axis and all distances are referenced to this point. When the rays emerge from the lens and enter air/vacuum, they are refracted towards the optical axis. Using Fermat's principle [21-23], the rays emerging from an arbitrary point P(x,y) on the lens interface will have traveled the same optical path distance in reaching the focal point as those rays which will have passed along the optical axis.

#2224 - $15.00 US Received March 13, 2003; Revised April 11, 2003

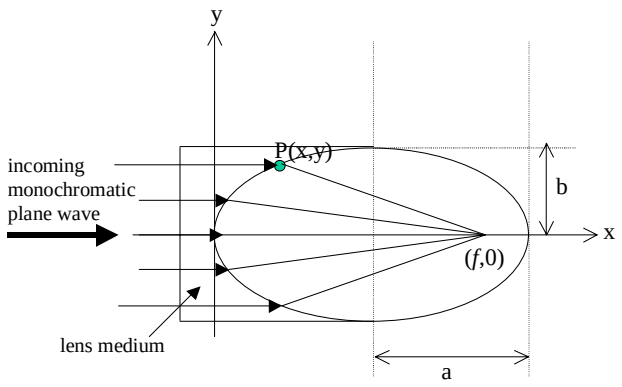

Fig. 2. A single planar concave lens. Incident parallel x-rays are brought to a focus at (F,0) due to the difference between the refractive indices of the lens medium and air/vacuum interface.

Equating optical path lengths, $n'x+\sqrt{(f-x)^2+y^2}=f$ and substituting for the real part of the refractive index gives, $y^2+(2\delta-\delta^2)x^2-2\delta fx=0$. This simply represents the functional form of an ellipse, where the half-lengths of the major and minor axes are, $a=\frac{f}{2-\delta}$ and $b=f\sqrt{\frac{\delta}{2-\delta}}$ respectively. As shown in Fig. 2, the ellipse has a maximum aperture of $2\times b$, where as that of a parabolic profile extends to infinity. It is clear that the parabolic shape is incorrect, for it is impossible for the lens to focus all rays along the infinitely extendable profile through refraction. The correctness of the elliptical shape is further substantiated by consideration of the deflection of the tangential ray at the lens vertex (a,b); using the small angle approximation and neglecting second-order terms in δ, this angle is simply the critical angle, $\theta \approx \frac{b}{f-a} \approx \sqrt{2\delta}$, a physically appealing result. A comparison between the parabolic and elliptical profiles with the same radii of curvature (475.5 nm) at the apex of the lens is shown in Fig. 3. Evidently, the profiles are close at the optical axis but diverge rapidly for larger lens apertures.

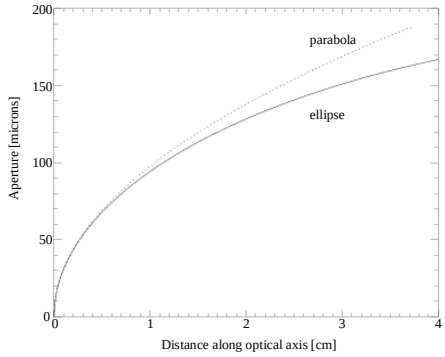

Fig. 3. Elliptical and parabolic profiles with the same radii of curvature at (0,0). The elliptical curve reaches a maximum at 7.5 cm, which determines the aperture of the system.

#2224 - $15.00 US Received March 13, 2003; Revised April 11, 2003

3. Ray-tracing simulations of single-element refractive lens

The SHADOW ray-tracing code [24-27] was used to assess the performance of a single solid elliptical lens (not a kinoform profile). Both parallel and divergent (synchrotron) illumination were considered. Ray-tracing simulations were performed on a refractive lens operating at 12.398 keV and with a focal length of 15 cm. This shape had the same elliptical parameters as those of the real fabricated lens (see below), but without the deletion of 2π phase-shifting regions. The elliptical parameters were: a ~ 7.5 cm, b ~ 189 μm and the radius of curvature was ~ 475.5 nm at the lens apex. For synchrotron radiation, the important parameters are the source size and distance from the electron source to the lens. For the National Synchrotron Light Source (NSLS) X13B Mini-Gap Undulator (MGU) [28,29] beamline, where the refractive lenses are to be installed, these are 15.5 μm *fwhm* (vertical source size) and 25 m respectively. Shown in Fig. 4. is the plot of the rays at the focal position (left) for divergent synchrotron radiation illumination, and the histogram of the rays through a vertical slice of the focused beam (right).

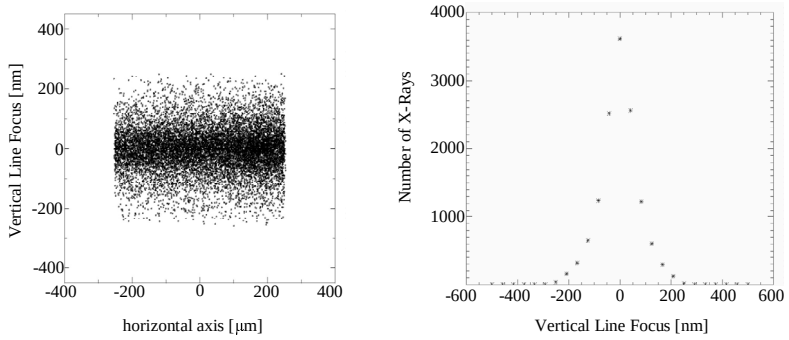

Fig. 4. (left) - Ray-tracing simulations of a solid single-element refractive lens. (right) - Histogram of a vertical slice through the line focus.

Ray-tracing simulations suggest that the x-rays are brought to a well-defined 130 nm *fwhm* line-focus. The demagnified source size is ~ 93 nm *fwhm* and the diffraction-limited resolution given by the Rayleigh resolution criterion is 113 nm *fwhm.* Adding these two values in quadrature gives a line-focus value of 146 nm *fwhm*, in close agreement with ray-tracing values. Furthermore, ray-tracing this lens with parallel ray illumination produced line-focus values which were almost identical to those obtained when divergent synchrotron radiation was used. This is understandable when one considers the maximum angle that the synchrotron x-rays make with the lens system. In our lens configuration, this value is only 15 μrad, and almost parallel to the optical axis.

4. Single-element refractive lens micro-fabrication

The process for fabricating the deep-etched x-ray micro-optics is as follows [30]. First, a plasma deposited thermal oxide mask layer (Tetraethylorthosilicate {TEOS}, 500 nm thick) is grown on clean silicon wafers (200 mm diameter, 875 μm thick). The chemically amplified resist, (UV113 - Shipley) was spun to a thickness of 400 nm and baked at 140 ^{o}C for 90 seconds. Patterns were written with an electron beam writer (JBX-9300FS) at 100 kV, and with a base dose of 50 μC/cm^2 that was modulated empirically to account for backscattered effects. A post-exposure bake of 90 seconds at 130^{o}C was followed by development in Tetramethyl Ammonium Hydroxide {TMAOH} solution (NMD-3 - Ohka) for 90 seconds and a rinse in water. After a spin-dry, the entire post-exposure process was subsequently repeated with a 20 second bake and a 30 second development step. The patterns were transferred to an oxide mask with an AMAT 5200 reactive ion etcher, using an EMAX plasma source for magnetically enhanced reactive ion etching, with a freon/oxygen etch chemistry. After the hard oxide mask was patterned, the remaining resist was removed and the remaining oxide

#2224 - $15.00 US Received March 13, 2003; Revised April 11, 2003

was used as a hard mask for the etching of the silicon. The deep silicon etch was a modified Bosch process and was performed in a specially designed, high throughput Advanced Silicon Etcher (ASE) which is the result of collaborative development with Agere Systems and Surface Technology Systems (STS). The lens patterns were etched to a depth of 40 μm.

5. Performance of single-element refractive lens

A single-element silicon elliptical refractive lens was fabricated for an x-ray energy of 12.398 keV and a focal length of f = 15 cm, with elliptical parameters as listed in Section 3. The focal properties of the lens were assessed at the NSLS (2.8 GeV, 200 mA) X13B MGU beamline. The lens was mounted on a rotation/translation stage (6 degrees of freedom) which was located on a heavy granite table, and was arranged to provide focusing in the vertical direction. A motorized Huber slit was placed before the lens to define the incoming x-ray dimensions (100 μm vertical and 10 μm horizontal). A scintillator crystal and lithographically patterned copper knife-edge were placed 15 cm from the lens on a diffractometer that had the required rotational/translational degrees of freedom. An incident x-ray energy of 12.398 keV was selected using a double-crystal Si(111) monochromator. Energy calibration of the monochromator was performed by measuring the position of the absorption edges of several EXAFS-standard thin foils. In addition, the upper crystal of the monochromator was detuned to reduce higher-order harmonic contamination. The lens was rotated until the best line focus was obtained visually using a charge-coupled device camera. The knife-edge was then scanned across the beam and the copper fluorescence was monitored to determine the focussed x-ray beam dimensions. The experiment was repeated for varying lens rotations, knife-edge positions and orientation, as well as incident x-ray photon energy.

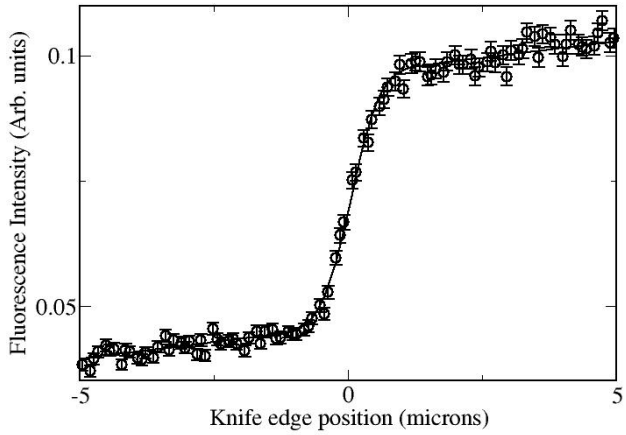

Fig. 5. Copper fluorescence Knife-edge scan taken on the refractive lens (shown in Fig.1).

Figure 5 shows the copper fluorescence counts as the lithographically patterned knife-edge is scanned through the focused x-ray beam in 0.1 μm steps. The Gaussian fit to the knife-edge scan is (1.0 ± 0.1) μm *fwhm* and is the smallest focussed hard x-ray beam measured at the NSLS. However, the expected value, adding the demagnified source size and diffraction-limited resolution in quadrature, is only 0.18 μm *fwhm*. We believe that the reason for the larger than expected measured result is due to limitations in the experimental set up. One major source of error could be the angular alignment of the knife-edge with the x-ray line focus, which was not well controlled. We note that for a knife-edge misalignment of 1 degree and a horizontal beam size of 40 μm, a 0.7 μm error will be added to the vertical beam size measurement. We will address this shortfall in the forthcoming experiments.

#2224 - $15.00 US Received March 13, 2003; Revised April 11, 2003

6. Discussion

Hard x-ray diffraction-limited refractive lenses can be manufactured using micro-fabrication techniques. However, the lens shape thus far has been parabolic [3,16,17,31]. In this article, we show that the ideal parallel-to-point lens profile for a single element is that of an ellipse. In addition, a single-element 2π phase-shifting Fresnel lens minimizes loss and enables short focal length devices to be manufactured.

One implication of the elliptical shape is that for a given focal length and refractive index, the diffraction-limited resolution given by the Rayleigh criterion $f\lambda/(\text{aperture}) = f\lambda/2b \sim \lambda/\sqrt{2\delta}$ is dependent only on the choice of material and the wavelength, even for a lossless material and in the refractive limit. For $\delta = 10^{-6}$ the diffraction-limited resolution is $\sim 10^{3}\lambda$. The above discussion is valid for a single element and by using more than one lens, this resolution limit can be exceeded.

A single-element with the minimum thickness reduces the energy deposited in the lens and makes them robust to the high heat loads present at synchrotron beamlines. This minimized loss also allows for larger lens apertures, and hence better resolution. Most fabrication techniques have a minimum feature size, and this minimum feature size has a direct correspondence to the focussed spot dimensions, just as for a zone plate. Increasing the feature sizes by introducing multiples of 2π phase-shifts can circumvent this limit. In this case the variation of loss within a single Fresnel zone will limit the resolution.

One major disadvantage of this optic is that it is produced by a planar technology, resulting in a line focus. To produce a spot, one simply uses a crossed pair of lenses [3], with the drawback that each optic introduces some loss. If it were possible to pattern and fabricate in 3 dimensions, rather than the 2 dimensional methods used here, one could use a single element to create a spot further reducing loss.

One difference between this type of kinoform optic and binary zone plates is that all of the elastically-scattered incident light is focused into a single spot, whereas the binary zone-plate also focusses light into higher orders, even for $\beta = 0$. These higher orders serve as a background and reduces the signal-to-noise ratio for imaging applications. A further advantage of these refractive lenses, in comparison to binary zone plates, is that they have a slight improvement in resolution for the same smallest feature manufacturing capability.

One aspect of these refractive lenses that is often overlooked, is that light at hard x-ray wavelengths are sensitive to the atomic structure of the lens medium. Any imperfections in crystal structure, such as grain boundaries, will provide a scattering contribution to the background signal and reduces the signal-to-noise ratio for imaging applications. We suggest single-crystal material for lens manufacture.

In summary, using micro-fabrication techniques we have manufactured a single-element kinoform lens in single crystal silicon with an elliptical profile for hard x-ray photons. By fabricating a lens that is optimized to operate at fixed wavelengths, absorption is significantly reduced. This allows a small radius of curvature at the lens apex, and high demagnification of a finite synchrotron electron source size through a shorter focal length. The reduced absorption loss also enables optics with a larger aperture, and hence improved resolution for focussing and imaging applications.

Acknowledgements

Research carried out at the National Synchrotron Light Source, Brookhaven National Laboratory, which is supported by the U.S. Department of Energy, Office of Basic Energy Sciences and Division of Materials Sciences under Contract No. DE-AC02-98CH10886. Micofabrication performed at the New Jersey Nanotechnology Consortium.

#2224 - $15.00 US Received March 13, 2003; Revised April 11, 2003